Analytical and Experimental Research of Vaporizer type Combustion Chamber of Expendable Turbojet

Nikola Davidović
Associate professor
University of Belgrade
Faculty of Mechanical Engineering

Branislav Jojić
Full Professor
University of Belgrade
Faculty of Mechanical Engineering

This paper presents analytical and experimental research on expendable turbojet combustion chamber with central-single vaporizer configuration. Expandable turbojet implies that engine is for single use and that simplicity and small size are dominant criteria. Because of these limitations it was considered that use of vaporizers instead of atomizers will save time needed for vaporization of the fuel. Most of empirical and experimental data related to combustion chambers origin from bigger engines and if we directly apply them to smaller combustors most likely we will overestimate their performances. That was one of important reasons for this research. Analytical analysis is based on ratio of vaporized fuel and ratio of residence time to droplet vaporization time with influence of geometry, working conditions and fuel type. Experimental analysis is focused on primary and secondary zone, its stability and efficiency. This paper combines analytical and experimental research of such space limited combustion chamber with central vaporizer.

Keywords: *combustion chamber, vaporizer, primary zone, turbojet, expendable*

1. INTRODUCTION

This paper presents research on expendable turbojet combustion chamber primary and secondary zone with - turbojet implicates that engine is for single use and that simplicity is dominant criteria. On the other hand these engines are small comparing to aircraft engines usually in range from 40 to 400 daN of thrust, so their dimen–sions and weight are in range of 150 to 400mm in dia–meter with weights from 4 to 70 kg [1]. Finally we may conclude that these engines generally don't have enough space for combustion chamber from two main reasons: maximum diameter is limited because of requirement for installation of engine into system and maximum length for combustion chamber is limited because of system length and, depending on certain design, bigger length of combustion chamber usually mean bigger distance between bearings which is causing problems with rotordynamic. That is why we have completely different approaches in the design of such combustors [2-4]. Because of these limitations it was considered to use vaporizers instead of atomizers to save time needed for vaporization of the fuel [5]. This paper presents research of such combustion chamber with central vaporizer with geometry configuration similar as [6].

Processes which are going on simultaneously in combustion chamber are fuel vaporization, fuel vapor and air mixing and chemical reaction [7]. Time needed for each of these processes is compared to air residence time in combustion chamber and then interpreted with engineering numbers. These engineering numbers which are used for calculation of combustion chamber effi–ciency and stability are based on ratio between time needed for chemical reaction and residence time. They are suggesting that other two processes, vaporization and mixing are not limiting the whole process. Usually that is truth because we are trying to make these processes complete by producing appropriate size of fuel droplets [8] and by organizing appropriate mixing, especially at design point. But desire to make size of combustor as smaller as possible and off design operations are bringing operation of combustors on the lower limits. This is specially case in small expendable engines [9]: the pressure ratios in these engines is in range from 3 to 6 while small dimensions are decreasing already small residence time. This research is dealing with such combustion chamber, by estimating proposed model and by experimental validation.

2. ANALYTICAL RESEARCH

Odgers [10] analyzed data from five different combus–tors, four with centrifugal atomizers and one with vaporizers, and found following criteria:

$$\log\left[\log\left(\frac{100}{\eta_g}\right)\right] = A\cdot\log\left[\frac{m_f}{P_c^n\cdot V}\cdot tk\left(\alpha,T_a\right)\right] + B\cdot\alpha^m + C\left(\alpha\right) \tag{1}$$

where η_g is combustion chamber efficiency, P_c-total pressure at combustion chamber inlet (bar), V-volume of the combustion chamber burning zone (m^3), m_f-fuel mass flow rate (kg/s,) α-coefficient of air excess, T_a-air

Received: Januar 2026, Accepted: March 2026
Correspondence to: Dr Nikola Davidovic
Faculty of Mechanical Engineering,
Kraljice Marije 16, 11120 Belgrade 35, Serbia
E-mail: ndavidovic@mas.bg.ac.rs
doi: 10.5937/fme2602234D

temperature (K), n and m exponents which are depen–ding on coefficient of air excess. More about coefficient of air excess could be found in [11] and [12].

Mathematical model for suitable geometry proposed in [13] is presented below. That mathematical model is based on characteristic times in the combustor and it is defined with following expression:

$$\eta_g^* = \left[p + (1-p)\cdot \tau_2 \right] \cdot \eta_g \tag{2}$$

where p≤1 is percentage of fuel vaporized in vaporizer, $\tau_2 \leq_1$ratio of residence time and time needed for droplet vaporization while η_g is efficiency from equation (1), with similar logic as [14] and [15].

Actually, during some preliminary testing it was obvious that the equation (1) is giving more optimistic prediction of the efficiency. Adding the influence of vaporized fuel and the atomizers role of the vaporizer we introduced correction to the equation (1).

Heat transfer in gas turbine combustor has been analyzed in a different ways such as in [16] and [17]

Percentage of vaporized fuel is calculated from ene–rgy balance: convective and radiative heat flux from primary zone are used to preheat liquid fuel, vaporize - vaporized fuel and air to final final temperature of the mixture exiting vaporizer, as presented in Eq. 3.

$$\begin{aligned} &(q_r + q_c)\cdot A_v = m_f \cdot \left[\int_{T_{gor}}^{T_{pi}} C_g(T)\,dT + \right. \\ &+ \int_{T_{pi}}^{T_{ii}} \frac{dp(T)}{dT} L_t(T)\,dT + \int_{T_{pi}}^{T_{ii}} \left[1 - p(T)\right]\cdot C_g(T)\,dT + \\ &\left. + \int_{T_{pi}}^{T_{ii}} p(T) C_{Ppg}(T)\,dT \right] + m_{ai} \cdot \int_{T_V}^{T_{ii}} C_{PV}(T)\,dT \end{aligned} \tag{3}$$

from which we may determine the temperature at the exit of the vaporizer and consequently the percentage of vapo–rized fuel p(T_{ii}). Labels in the equation (3) are: q_r and q_c radiative and convective heat flux (W/m^2), A_v-vaporizer heated surface (m^2), T_{gor}-fuel temperature (K), T_{pi}- tempe–rature of fuel start of vaporization (K), T_{ii}-vaporization (J/kg), C_g-liquid fuel specific heat (J/kgK), C_{Ppg}-fuel vapor specific heat (J/kgK), C_{PV}-air specific heat (J/kgK) and m_{ai}-air mass flow rate through vaporizer (kg/s) [13].

Equation (3) assumes that the two phase mixture is at the same temperature i.e. air, vaporized and non-vaporized fuel are at the same temperature. In reality there will be value of the percentage of the vaporization according to equation (3) gives good estimation of the process.

From the equation (3) we may conclude that the per–centage of the vaporized fuel depends on geometry of vaporizer and combustion chamber, mixture ratio in the vaporizer and primary zone, type of the fuel, inlet temperature of the fuel and air but also depends on apsolute fuel flow rate! Because the temperature of the air depends on compressor and the whole turbojet it is logic to consider certain fuel type for the certain turbojet.

Residence time in the primary zone can be written as

$$t_R = \frac{M_g}{m_{aprim} + m_f} = \frac{\rho_g \cdot V_{prim}}{m_{aprim} + m_f} \tag{4}$$

where M_g-is the mass of gases in the primary zone (kg), ρ_g-density of gases in the primary zone (kg/m^3) and V_{prim} is the volume of primary zone (m^3).

If we use expressions for the density and continuity equation we may write

$$\begin{aligned} &\rho_g = \frac{P_c}{R_g \cdot T\left(\alpha_{prim}, \eta_g\right)} \text{ and} \\ &m_{aprim} + m_f = \frac{P_c \cdot A_c}{C^*} = \frac{P_c \cdot A_c}{\frac{\sqrt{R_g \cdot T\left(\alpha_{prim}\cdot \eta_g\right)}}{\Gamma(Kg)}} \end{aligned} \tag{5}$$

where R_g is gas constant (J/kgK), α_{prim} is coefficient of air excess in primary zone, $m_{aprim}$is air flow rate through primary zone (kg/s), A_c-critical cross section of the nozzle (m^2), C^*-characteristic velocity (m/s) and $\Gamma(\kappa_g)$-function of ratio of specific heats at constant pressure and volume[13].

Combining with equation (4) we have

$$\begin{aligned} t_R &= \frac{V_{prim}}{A_{kr}} \cdot \frac{1}{\Gamma(Kg)\cdot\sqrt{R_g \cdot T\left(\alpha_{prim}\cdot\eta_g\right)}} = \\ &= \frac{L^*}{\Gamma(Kg)\cdot\sqrt{R_g \cdot T\left(\alpha_{prim}\cdot\eta_g\right)}} \end{aligned} \tag{6}$$

where L^* is ratio of volume to critical cross section known from rocket propulsion as characteristic lenghth. From equation (6) it can be seen that residence time, at defined working conditions (pressure, temperature and air flow), depends on geometry and fuel properties because fuel to air ratio defines adiabatic temperature and gas properties.

Now the ratio of the droplet residence time in the primary zone and time needed for droplet vaporization could be expressed as

$$\tau_2 = \frac{t_g}{\tau_{ik}} = \frac{\frac{L^*}{\Gamma(Kg)\cdot\sqrt{R_g \cdot T\left(\alpha_{prim}\cdot\eta_g\right)}}}{\frac{D_o^2}{k}} \tag{7}$$

where D_o is the initial droplet diameter (m) and κ is the vaporization constant (m^2/s) [8].

Final efficiency is then calculated by iteration of eq. 2 because all parameters depend on efficiency.

Simplified model is shown at Figure 1. Vaporizer is in the center of annular combustor, fuel is injected in vaporizer. Part of the air of primary zone goes through vaporizer, the rest enters from the holes at liner. The geometrical values which will be used in mathematical model are shown: length of vaporizer-lk and primary zone-lprim, diameter of vaporizer-dgi and primary zo–ne-dgi and that was the geometry to be optimized [18].
The proposed correction is based on logic that the percentage of the vaporized fuel and atomization quality of the vaporizer are limiting the proces in small turbojets, where volume (or residence time) and air pressure and temperature (time needed for chemical reaction) are lower than in conventional turbojets.

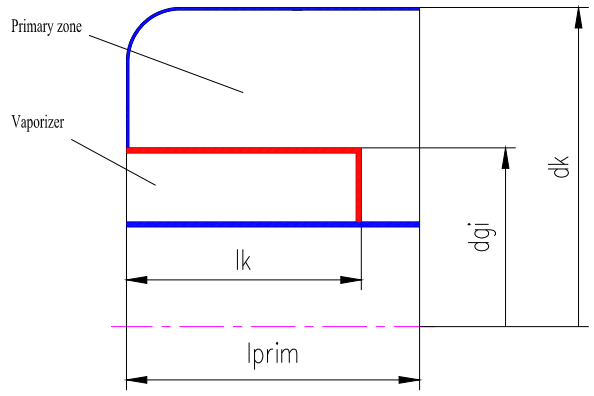

Figure 1. Geometrical labels

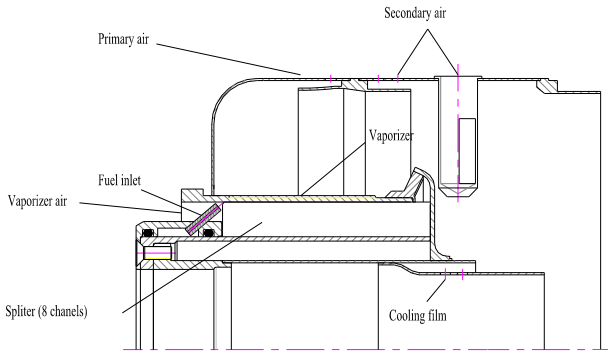

Figure 2. Combustor primary and secondary zone

Quality of the process is analytically analyzed through infuences of:

-Air pressure and temperature (regime 1 and 2)
-Air to fuel mixture ratio in primary zone
-Air flow ratio of the flows through vaporizer and primary zone
-Geometry of the vaporizer and combustor
-Fuel type

This research is related to the combustion chamber of the certain turbojet engine and consequently there are exact technical requests:

-Maximum diameter of combustion chamber casing Dmax=155mm
-Maximum length of combustion chamber Lmax=150mm
-Design point conditions (regime 2):
-air flow rate ma=0.8kg/s
-Total pressure Pc=2.8bar
-Total temperature Ta=423K
-Starting conditions (regime 1):
-air flow rate ma=0.4kg/s
-Total pressure Pc=1.4bar
-Total temperature Ta=323K

2.1 Analysis of the mass ratio of the vaporized fuel

At the figures 3-6 it is shown percentage of the vaporized fuel as a function of primary zone excess of the air coefficient for different ratios of air flows through the vaporizer and through the primary zone. If the fuel type is not mention than it is gasoline. At the figures 7-11 it is shown percentage of the vaporized fuel as a function of the ratio of air flow rates through the vaporizer and primary zone and as a function of lenght and diameters of primary zone and the vaporizer.

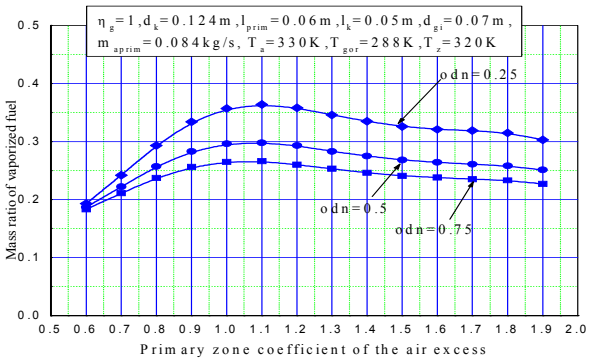

Figure 3. Mass ratio of the vaporized fuel as a function of primary zone coefficient of the air excess for different ratio of the air flows through vaporizer and primary zone, gasoline, regime 1

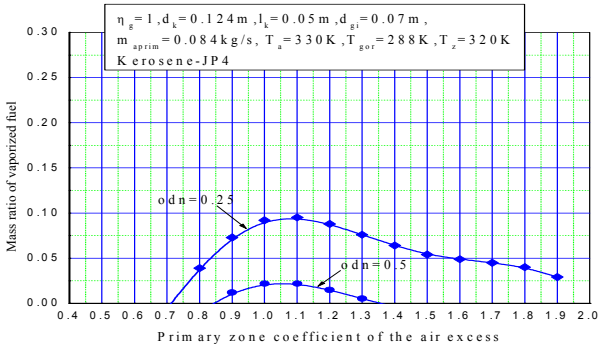

Figure 4. Mass ratio of the vaporized fuel as a function of primary zone coefficient of the air excess for different ratio of the air flows through vaporizer and primary zone, kerosene JP-4, regime 1

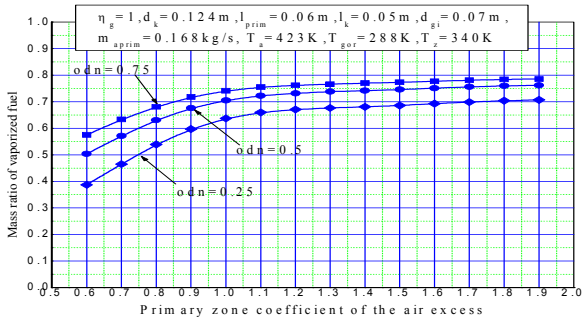

Figure 5. Mass ratio of the vaporized fuel as a function of primary zone coefficient of the air excess for different ratio of the air flows through vaporizer and primary zone, gasoline, regime 2

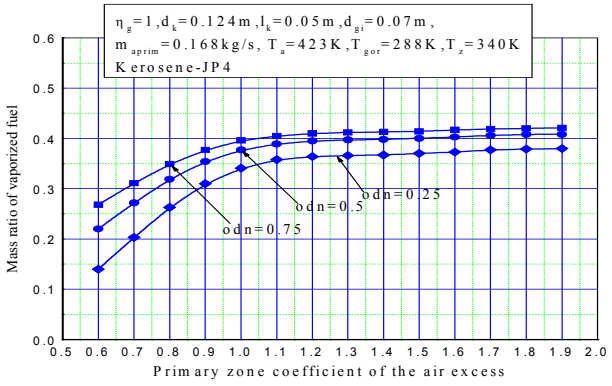

Figure 6. Mass ratio of the vaporized fuel as a function of primary zone coefficient of the air excess for different ratio of the air flows through vaporizer and primary zone, kerosene JP-4, regime 2

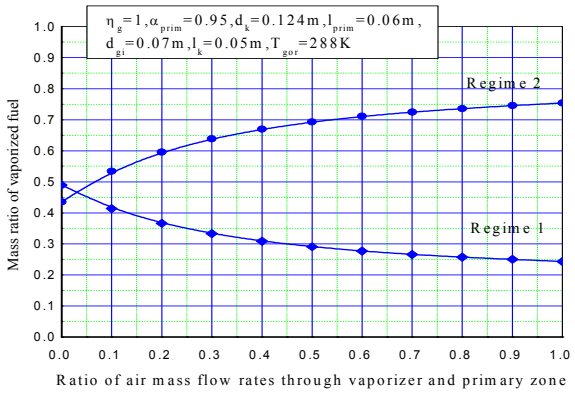

Figure 7. Mass ratio of the vaporized fuel as a function of ratio of the air flow rates through vaporizer and priamary zone of the coefficenct of the air excess in primary zone equals 0.9, fuel gasoline

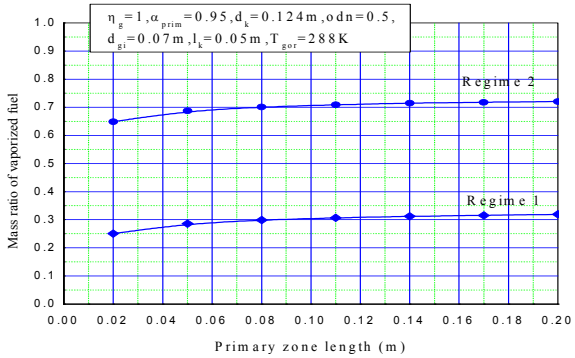

Figure 8. Mass ratio of the vaporized fuel as a function of primary zone length, coefficient of the air excess in the primary zone 0.95, fuel gasoline

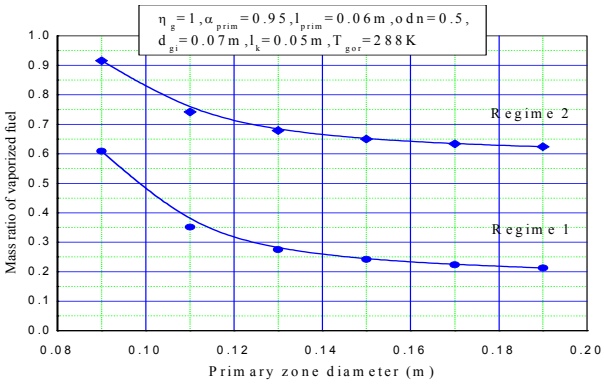

Figure 9. Mass ratio of the vaporized fuel as a function of primary zone diameter, coefficient of the air excess in the primary zone 0.95, fuel gasoline

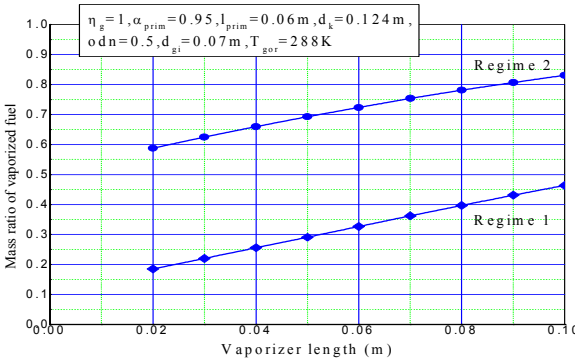

Figure 10. Mass ratio of the vaporized fuel as a function of vaporizer length, coefficient of the air excess in the primary zone 0.95, fuel gasoline

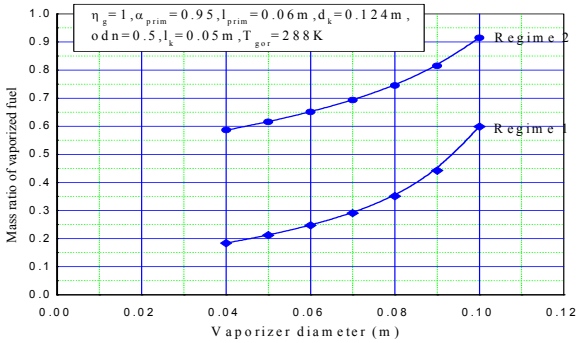

Figure 11. Mass ratio of the vaporized fuel as a function of vaporizer diameter, coefficient of the air excess in the primary zone 0.95, fuel gasoline

From previous figures we may conclude:

1. At the figures 3 and 5mass ratio of vaporized fuel is presented as a function of primary zone coefficient of air excess. The fuel is gasoline. At the regime 1 decrease of vaporizer air flow shifts the maximum to the lean areas while at the regime 2 maximum is not reachable while effect of air flow ratio through the vaporizer and primary zone influence is reversed due to higher air temperature.
2. At the figures 4 and 6 are shown the same curves with kerosene JP-4 as a fuel. The amount of vaporized fuel is lower while character of the curves is the same. Ratio of vaporization is lower while character is the same as with gasoline. At the regime 1 at air flow ratios of 0.75 the equilibrium temperature is below JP-4 starting evapo–ration temperature and consequently there is no vapori–zation. It means that the regimes of engine has to be in line with fuel type or concept of the combustion chamber. If we plan to use fuel with even higher temperature of evaporation the use of the vaporizer will be questionable.
3. Air ratio has different influence to the vaporized fuel as shown at the Figure 7. It seams that for given cases optimum ratio is about 0.5. Also, it would be interesting if we can control the air ratio, i.e. to keep low values at the regime 1 and to increase that ratio at the regime 2!
4. Lenght of the primary zone has small effect and only through increased volume and concequently radiative heat flux. From the Figure 8 it is obvious that the length of primary zone should not be increased due to vaporization reason.
5. At the Figure 9 is shown the effect of the primary zone diameter. The smaller diameter is increasing vaporization because of the increase of the velocities in the primery zone and concequently convective heat flux. Howeverm that influence should be considered together with air loading of the primary zone because increase in the velocity could significantly effect residence time and stability at all.
6. Figure 10 shows the effect of the vaporizer length. It is generally linear dependance because it increases the heat transfer surface. Again, the lenght of the vaporizer should be considered having in mind the complete flow picture in the primary zone.
7. The same trend but parabolic is shown at the Figure 11 where the effect of the vaporizer diameter is shown. Increase in vaporizer diameter also has same effect as decreasing the diameter of the primary zone i.e. increases convective heat flux but decreasing the reesidence time, so optimum has to consider that influence as well.

2.2 Analysis of the parameer τ2

It is logic to conclude that when residence time is smal–ler than time needed to vaporize the droplet the infuence of the parameter τ_2 is significant. Initial droplet diameter defines vaporizer as atomizer, in this case as airblast atomizer. On another side, the atomizer function depe–nds on fuel type, fuel to air ratio, ari velocity and finally, the geometry. From the equation (4) we may calculate the needed droplet diameter but it is the question could vaporizer make such small droplet. If not, than we have to increase characteristic length i.e. residence time.

At the Figures 12-22 are shown the effects of the primary zone coefficient of the air excess, droplet diameter, length and diameter of the primary zone and the vaporizer on the parameter τ_2.

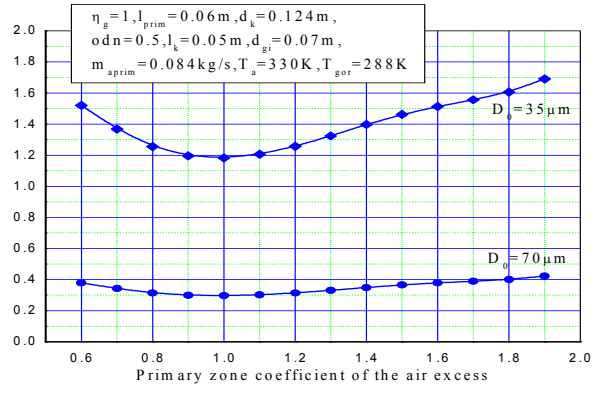

Figure 12. Parameter τ2 as a function of primary zone coefficient of the air excess for droplet diameters35 i 70μm, regime 1

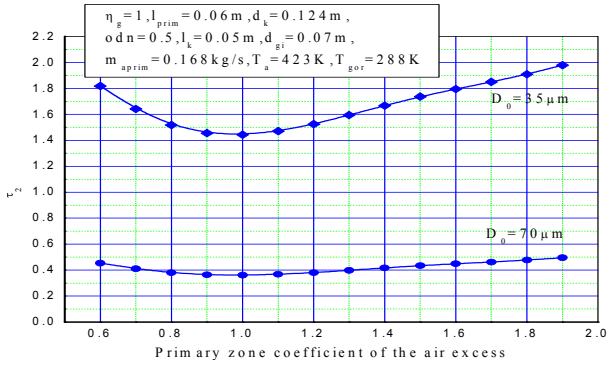

Figure 13. Parameter τ2 as a function of primary zone coefficient of the air excess for droplet diameters35 i 70μm, regime 2

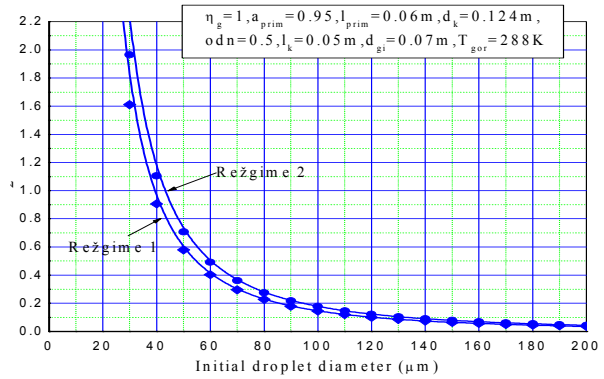

Figure 14. Parameter τ2 as a function of droplet diameter, for the primary zone coefficent of the air excess 0.95

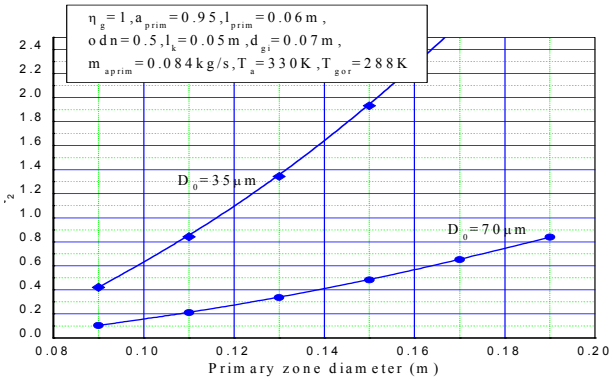

Figure 15. Parameter τ2 as a function of priamary zone diameter at primary zone coefficient of the air excess 0.95, for droplet diameters35 i 70μm, regime 1

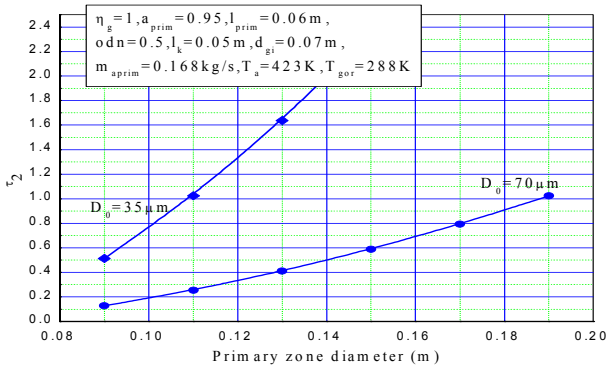

Figure 16. Parameter τ2 as a function of priamary zone diameter at primary zone coefficient of the air excess 0.95, for droplet diameters35 i 70μm, regime 2

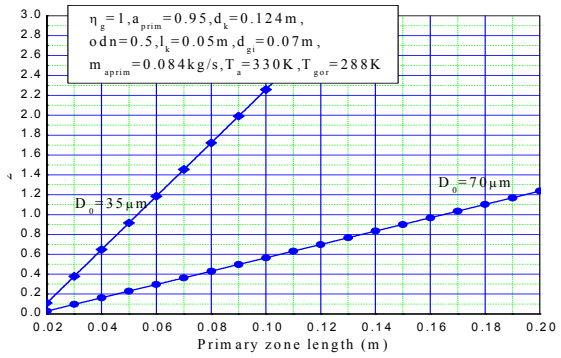

Figure 17. Parameter τ2 as a function of priamary zone length at primary zone coefficient of the air excess 0.95, for droplet diameters35 i 70μm, regime 1

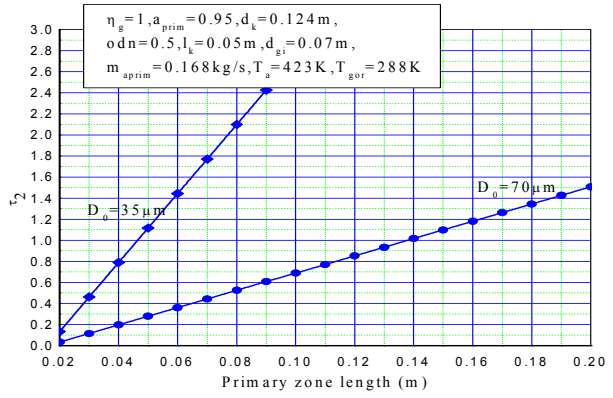

Figure 18. Parameter τ2 as a function of priamary zone length at primary zone coefficient of the air excess 0.95, for droplet diameters35 i 70μm, regime 2

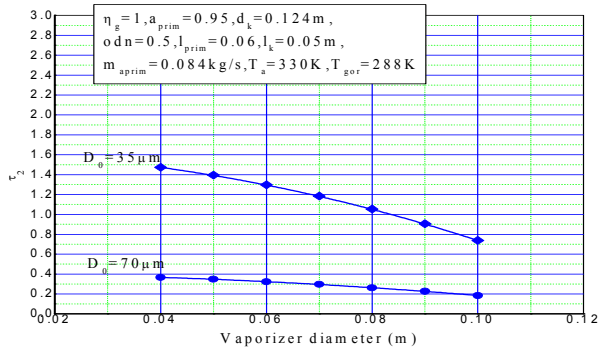

Figure 19. Parameter τ2 as a function of vaporizer diameter at primary zone coefficient of the air excess 0.95, for droplet diameters35 i 70μm, regime 1

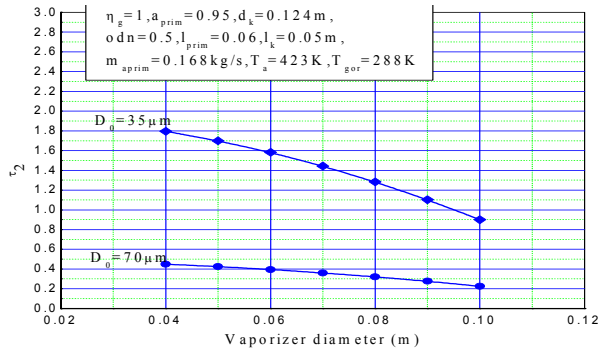

Figure 20. Parameter τ2 as a function of vaporizer diameter at primary zone coefficient of the air excess 0.95, for droplet diameters35 i 70μm, regime 2

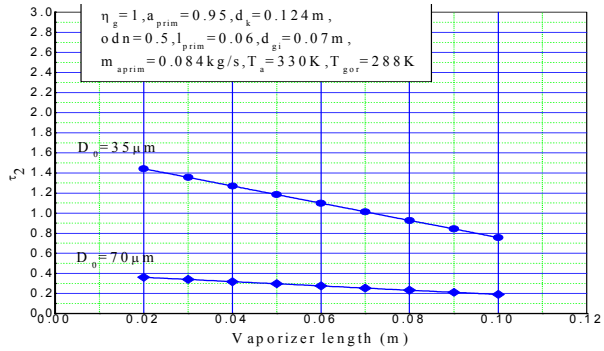

Figure 21. Parameter τ2 as a function of vaporizer length at primary zone coefficient of the air excess 0.95, for droplet diameters35 i 70μm, regime 1

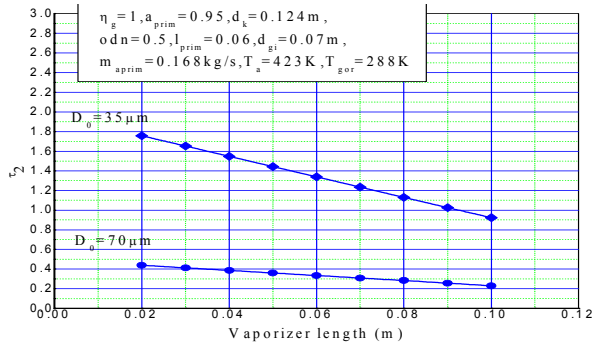

Figure 22. Parameter τ2 as a function of vaporizer length at primary zone coefficient of the air excess 0.95, for droplet diameters35 i 70μm, regime 2

From previous figures we may conclude:

1. Dependance of parameter$\tau_2$of primary zone coef–ficient of the air excess is shown at the Figures 12 and 13. If we assume that evaporation constant is inde–pendant of mixture ratio, the parameter τ_2 has minimum at the minimum residence time (maximum temperature). At the regime 2, the residence time is smalller but energy from primary zone is higher which gives better values for the regime 2. Also, the influence of the droplet diameter is very strong i.e. we have to consider the atomizer role of the vaporizer.
2. At the Figure 14 is underlined the effect of the initial droplet size. It has to be greater than 50μm for the re–gime 1, and greater than 40μm for the regime 2.
3. With increase in diameter and length of the primary zone we are increasing the residence time and consequently parameter τ2, lineraly with length and parabolically with diameter. The smaller the initial droplet size the bigger is the curve gradient. It is shown at the Figures 15-18.
4. The reverse influence but from the same reason is shown at theFigures 19-22 where parameter $\tau_2$is analy–zed as a function of vaporizer diameter and length.

3. EXPERIMENTAL RESEARCH

In order to verify presented analysis it was needed to experimentaly verify the conclusions [19]. Tests were focused on the primary and secondary zone because of previous analysis and because of its importance on behaviour of complete combustor [20]. Several types of tests were performed but measuring conditions were related to engine where combustor is intended to use. These conditions are:

Regime 1: m_a=0.4kg/s, T_a=323K and P_a=1.4bar

Regime 2: m_a=0.8kg/s, T_a=423K and P_a=2.8 bar

Also, several types of fuel were used: gasoline (standard engine unleaded gasoline 95), gasoline 80/120 and kerosene JP-4 [21] with no attempt to have similiarity conditions as in [22].

3.1 Testing of primary and secondary zone stability map

Stability map was determined with testing of combustor primary and secondary zone. Tests were performed with gasoline and with air inlet temperature of 323K (regime 1). Map is presented in coordinates of air flow rate and coefficent of the air excess in the primary zone. At the map are shown equivalent points (in terms of velocities and air to fuel ratio) of engine's steady state and acceleration line [23].

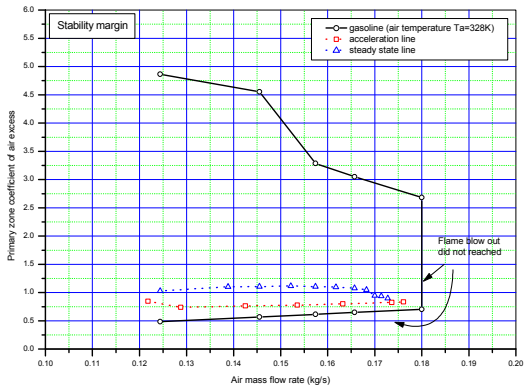

Figure 23. Primary and secondary zone stability map

Air distribution of combustor is previously tested (cold runs) and such distribution was used to determine the air to fuel ratios. During stability testing it was also determined the ignitionability. It is generally in offset of 0.3g/s comparing to the stability and the maximum flow rate for ignition was determined as 5g/s.

3.2 Visual examination of primary and secondary zone optimal regimes

During determination of the stability map it was decided to record flow regimes when the flow picture was visu–ally marked the best since the combustor was open. More than this, visualisation is always important information about the process in the combustor [24]. These regimes and these flow pictures are then compared to stability map and further to measurement of the efficiency.

It was also measured temperature of the mixture at the vaporizer exit as a function of the actuall coefficent of the air excess in the primary zone.

Then the air flow of the vaporizer and of the rest of the combustor was physically separated in order to estimate the influence of the ratio of the air flows of the vaporizer and primary zone. The fuel was gasoline.

Figure 24 is showing the temperature at the exit of the vaporizer as a function of primary zone coefficient of the air excess. At the Figure 25 is shown visually the optimum ratio of the air flows of the vaporizer and of the primary zone as function of the fuel flow rate. At the Figure 25 is shown picture of one of the point from Figure 24.

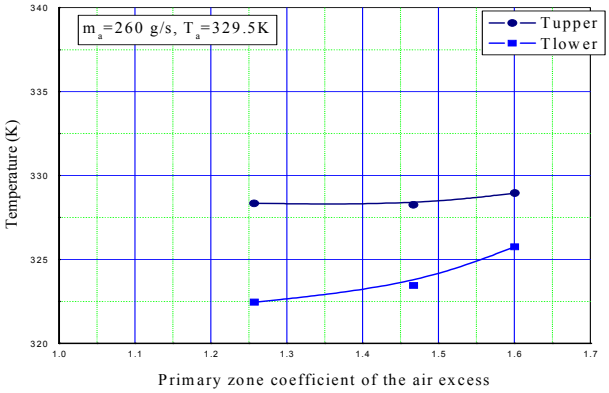

Figure 24. Temperature of the mixutre at the vaporizer exit as a function of primary zone coefficent of the air excess, upper and lower half respectively

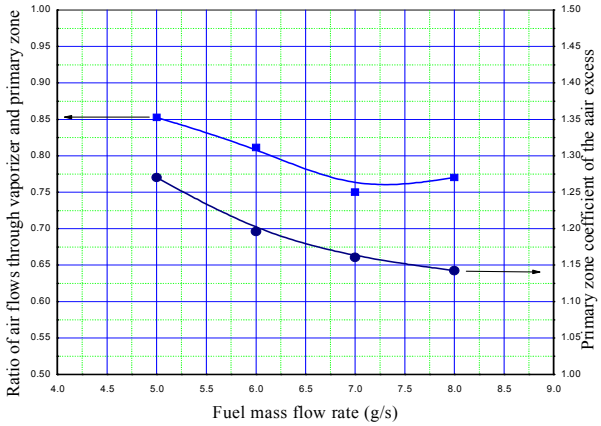

Figure 25.Visually optimum regimes

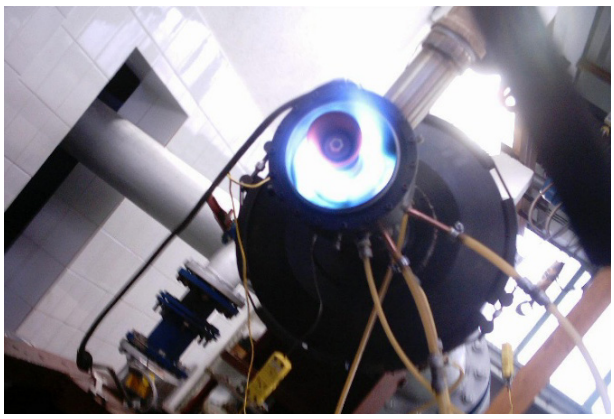

Figure 26.Photo of the test of the primary and secondary zone visual examination

3.3 Testing of primary and secondary zone efficiency

Tests of primary and secondary zone efficiency were performed with additional nozzle at the exit. The pur–pose of the nozzle is to simulate the back pressure and to calculate the efficiency as presented in [22]. This method is oftent used in rocket propulsion in order to estimate losses of characteristic velocity. The additional nozzle was cooled with water. The comparison with empirical values was intend to compare with test, no attemp was to use methods as in[25].Results are shown at the Figures 27-30.

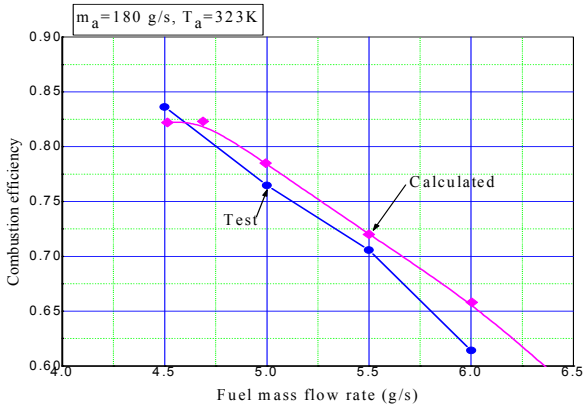

Figure 27. Efficiency of the primary and secondary zone as a function of fuel flow rate, fuel gasoline

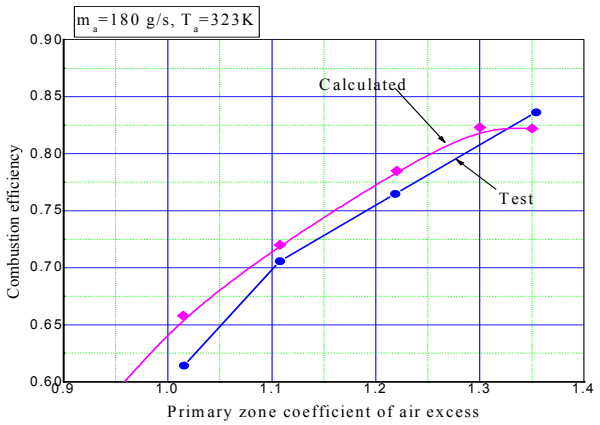

Figure 28. Efficiency of the primary and secondary zone as a function of primary zone coefficient of the air excess, fuel gasoline

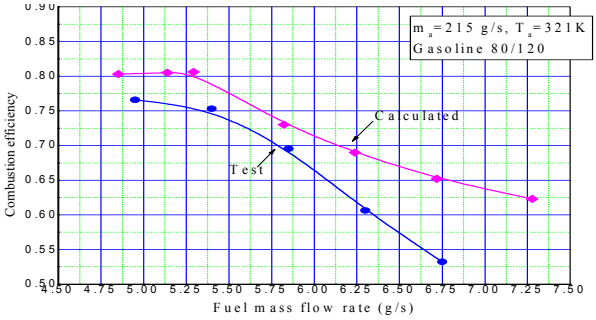

Figure 29. Efficiency of the primary and secondary zone as a function of fuel flow rate, fuel gasoline 80/120

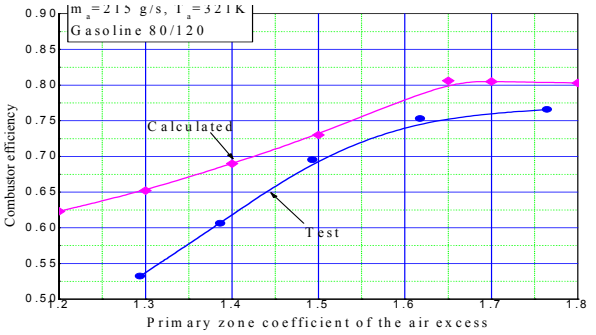

Figure 30. Efficiency of the primary and secondary zone as a function of primary zone coefficient of the air excess, fuel gasoline 80/120

From previous figures we may extract following conclusions:

1. At the Figures 27 and 28 are shown experimental and analythical dependance of primary and secondary zone efficiency versur fuel flow rate and coefficient of the air excess. Experimental curve is not showing maximum in tested area while analythical curve shows decrease after value of 1.3 of the coefficient of the air excess.
2. At the Figures 29-30 are shown the same dependance with gasoline 80/120. Both curves have the optimum at the lean side around value of 1.7 of the coefficient of the air excess while in the reach area there are differencies between experimental and analythical curve because these points were very close to the stability limit.

Analythical curves were calculated from equation (2) with correction coefficients a=1,b=0.75 i c=0.85. Because the mass ratio of the vaporized fuel and parameter τ_2 were calculated with assumption of efficiency equal to 1 we had to find the efficiency by solving following expression

$$\eta_g = \left\{a\cdot p(\eta_g,...)+\left[1-a\cdot p(\eta_g,...)\right]\cdot b\cdot \tau_2(\eta_g,...)\right\}\cdot \frac{c}{10^{A\cdot\log\left[\frac{m_f}{P_c^n\cdot V_{prim}}\cdot tk(\alpha_{prim},T_a)\right]+B\cdot\alpha_{prim}^{\,m}+C(\alpha_{prim})}}$$

Coefficients that are uses are shown in the Table 1.

Table 1. Experimental coefficients

/	*a*	*b*	*c*	*A*	*B*	*C*	*m*	*n*
$0.5\leq \alpha_{prim}<1$	1	0.75	0.85	0.91	-1.1	-0.89	1	$2\alpha_{prim}$
$1\leq \alpha_{prim}<2$	1	0.75	0.85	0.91	-1.1	-1.64	-1	$2/\alpha_{prim}$

3.4 Testing installation

Here is the short description of the testing Laboratory and air installation used for combustor testing. Laboratory has classic solution, i.e. electric motor together with multiplicating gear box for compressor testing and water cooled brake unit together with reducing gear box for turbine testing. Source of air is water cooled screw compressor of capacity 1kg/s of air at 10 bars. This plant is appropriate for turbine and turboshaft power up to 150kW, compressor power up to 150kW and turbojet thrust up to 500daN.

Laboratory scheme is shown at the Figure 31. Screw compressor (C1) is supplying air to the laboratory. Capacity is 1kg/s at 10 bar. Electric power required is 400kW. There are two lines from the compressor. Main line is supplying air online to the tested components or engines through valve (1). Auxiliary line is supplying air to reservoir (R) and can be used optionally through valve (18). Main line is passing through pipes with nominal diameter of 200mm (DN200). Overall mass flow rate is measured at flowmeter (1). An auxiliary combustion chamber (3) is used as air heater in order to increase air temperature before testing object (combus–tion chamber, turbine…). Then the main line is divided to direct (DN200) and by-pass line (DN100), both of these lines are controlled by motor-driven valves (4, 6). Position 5 is reserved for testing objects such as com–bustion chamber, intake, nozzle, turbojet engine wind–milling condition or ramjet. Amount of by-pass air is measured at flowmeter (7) and it can be adjusted with motor-driven valve (8). When turbine is tested then line starting with motor-driven valve (9) is opened. Turbine is connected to the brake (Br) through elastic-safety clutch (11) and reducing gear-box (Rd).

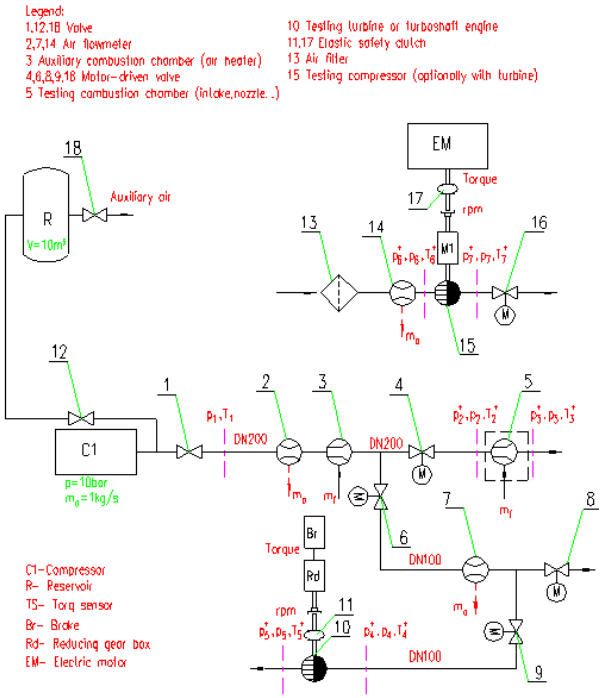

Figure 31. Laboratory scheme

Compressor is tested with electric motor (EM) through safety clutch (17) and multiplying gear box (M1). An air filter (13) should be positioned before

compressor intake. An artificial compressor intake (14) is used to measure air mass flow rate through compressor. Air mass flow rate through compressor is maintained with motor-driven valve (16) after compressor exit. In order to test turboshaft engine brake unit is used but only there is no need for air from installation. Typical measuring stations are also shown at the Figure 31 while characteristic photos are shown at the Figures 32,33,34 and 35.

Figure 32. Air compressor C1 from the Laboratory scheme

Figure 33. Details of air installation, elements 1, 2 and 3 from the Laboratory scheme

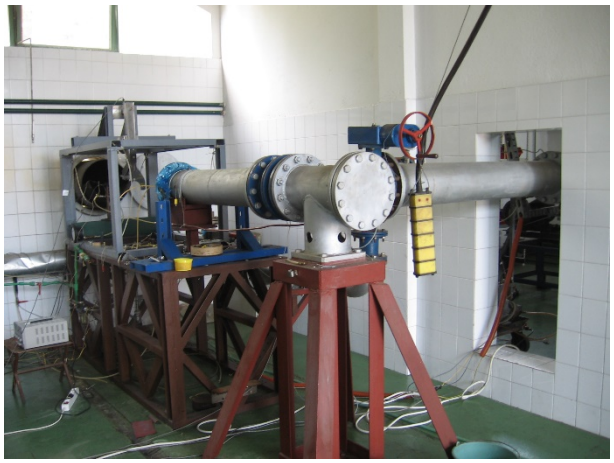

Figure 34. Details of air installation, elements 4, 6 and the line to the object 5 from the Laboratory scheme

Fuel installation is detaily described in [11]. At the figure 36 is shown configuration of primary and secon–dary zone for the atmospheric testing and its measuring points. At the figure 37 is shown configuration with nozzle at the exit.

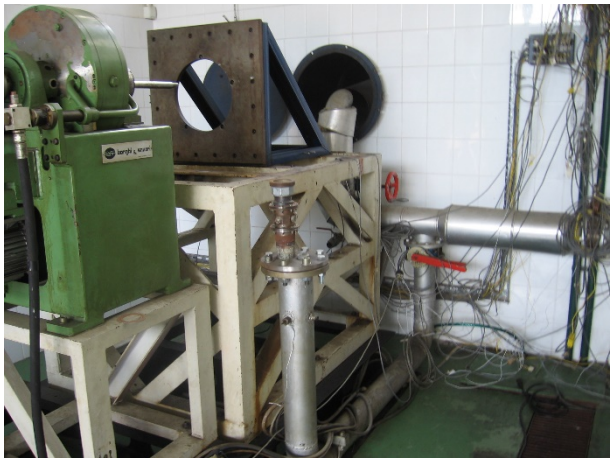

Figure 35. Details of air installation, elements 8, 9 and the brake unit from the Laboratory scheme

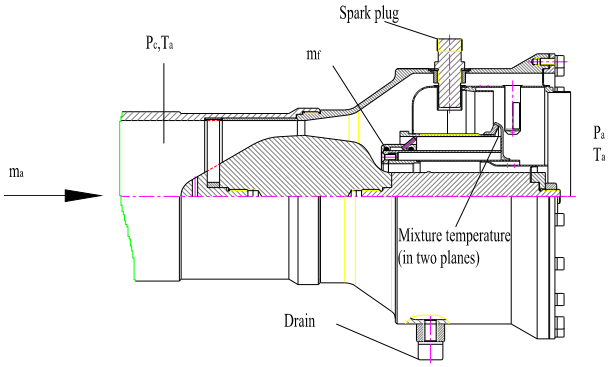

Figure 36. Measuring points for testing at atmospheric pressure

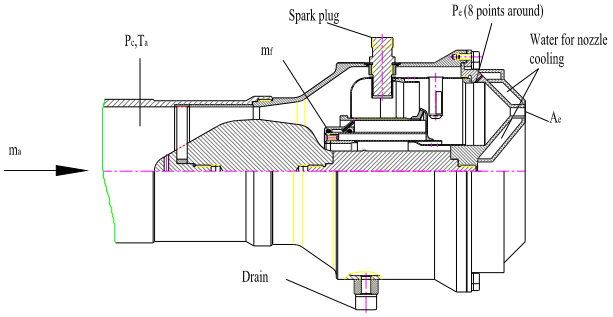

Figure 37. Measuring points for testing at working pressure

4. CONCLUSION

The analythical method for improvement of existng em–pirical efficiency correlation is analyzed and compared with test results. Existing models for efficiency estima–tion are based on combustors from bigger gas turbine engines which means bigger pressure and temperature, bigger volume, higher available pressure for atomi–zation etc. The analythical method introduced two parameters, mass fraction of vaporized fuel-p and ratio of residence time and time needed for chemical reaction τ_2. It was shown that correction is very significant for the regimes with low air pressure and temperature i.e. especially at starting regimes which is general weak point of vaporizers.

The main contribution of this work that it offers experimentally verified correction which could be used in similar combustors or similar analythical aproach could be used for different geometrical values, for example not single but several vaporizers. Vaporizer was analyzed not separately but as a part of the whole combustor system. It was shown analyticaly, experimentaly and visually that there are limiting coefficient of the air excess in the primary zone. It was also shown that there is significant effect of the fuel type at the efficiency of such combustors due to vaporizing characteristic which lead to use of more suitable fuel or fuel mixture for such combustors. It can be also concluded that the atomizing effect of the vaporizer can not be neglected, always part of the fuel will vaporized but the rest has to be properly atomized so the vaporizer should act as atomizer as well.And finally, the visual test shown the good agreement with best efficiency regimes underlying the importance of test and visualisation of the process.

ACKNOWLEDGEMENT

The authors wish to acknowledge and to thank the company EDePro – Engine Design and Production from Belgrade, Serbia for their support in the realization of this project, especially from their experience with design, production and testing of turbojet engine TMM-40. Research of this paper is also result of the national project financed by Serbian Ministry of Science, Technological Development and Innovations (contract 451-03-34/2026-03/ 200105 from 05.02.2026.).

REFERENCES

[1] N. Davidovic, M. Milos, B. Jojic, Development of an Expendable Turbojet Engine for the Propulsion of an Unmanned Aerial Vehicle, FME Transactions Vol. 53, No 4,2025.

[2] C.E. Smith, E.J. Fuller, D.S. Crocker, Dual Spray Airblast Fuel Nozzle for Advanced Small Gas Turbine, Journal of Propulsion and Power, Volume 11, Issue 2, May 1995.

[3] M.J. Melo, M.M. Sousa, M. Costa, Y. Levy, Experimental Investigation of a Novel Combustor Model for Gas Turbines, Journal of Propulsion and Power, Volume 25, Issue 3, May/June 2009.

[4] B. Ariabatar, R. Koch, H.J. Bauer, D.A. Negulescu, Short Helical Combustor: Concept Study of an Innovative Gas Turbine Combustor with Angular Air Supply, Journal of Engineering for Gas Turbines and Power, GTP-15-1291, March 2026.

[5] A. Sotheran, The Rolls-Rouce Annular Vaporizer Combustor, Journal of Engineering for Gas Turbines and Power, January 1984.

[6] В.Н. Афросимова, Е.И. Козельский, С.А. Волошин, Small Film-Evaporating Combustor for small Gas Turbines (translate from russian) , Aviation Technic, 1986/1

[7] A.H. Lefebrve, Gas Turbine Combustion, Hemisphere Publishing Corporation, 1986.

[8] A.H. Lefebrve, Atomization and Sprays, Hemisphere Publishing Corporation, 1989.

[9] A. Bodemer, World Aviation Engines(translation from french), Editions Lariviere, 1979.

[10] J. Odgers, C. Carrier, Modeling of Gas Turbine Combustors; Considerations of Combustion Efficiency and Stability, Journal of Engineering for Power, April 1973.

[11] N. Davidović, N. Kolarević, M. Stanković, M. Miloš, Research of expendable turbojet tubular combustion chamber, Advances in Mechanical Engineering, Vol. 14, Issue 5, 2022. (ISSN 1687-8140)

[12] V.Fotev, Airbreathing propulsion (translation from serbian), Faculty for Mechanical Engineering University of Belgrade, Belgrade, 2010.

[13] N. Davidović, Mathematical model of the turbojet engine combustion chamber primary zone, FME Transactions (ISSN 1451-2092),, Vol. 35, No 1, 2007.

[14] P.A. Leonard, A.M. Mellor, Correlation of Gas Turbine Combustor Efficiency,Journal of Energy, 1982.

[15] C. Hargreaves, P. Denman, D. Franc, I. Mariah, J.F. Carrotte, A.D. Walker, Characteristic Time Scale Modeling of Gas Turbine Combustor Ignition Limits at Sub Idle Conditions, Journal of Engineering for Gas Turbines and Power, GTP-25-1484, May 2016.

[16] P.J. Stutaford, P.A. Rubini, Assesment of a Radiative Heat Transfer Model for Gas Turbine Combustor Preliminary Design, Journal of Propulsion and Power, Volume 14 , Issue 1, January 1998.

[17] R. Shiele, S. Wittig, Gas Turbine Heat Transfer: Past and Future Challanges, Journal of Propulsion and Power, Volume 16, Issue 4, Jul 2000.

[18] B.S. Mohammad, J. Cai, S.M. Jeng, Gas Turbine Combustor Flow Structure Control Through Modification of the Chamber Geometry, Journal of Engineering for Gas Turbines and Power, September 2011.

[19] H.E. Bower, A. Schwarzle, F. Grimm, T. Zornek, P. Kutne, Experimental Analysis of a Micro Gas Turbine Combustor Optimized for Flexible Operation with Various Gaseous Fuel Composition, Journal of Engineering for Gas Turbines and Power, GTP-19-1427, March 2020.

[20] S. Gogineri, D. Shouse, C. Frayne, J. Sutrud, G. Sturgess, Combustion Air Jet Influence on Primary Zone Characteristics for Gas Turbine Combustors, Journal of Propulsion and Power, Volume 18, Issue 2, May 2002.

[21] Coordinating Research Council, Handbook of Aviation Fuel Properties, Atlanta, September 1983.

[22] V. Fotev, Similarity Criterions for Liquid Propellants, FME Transactions., Vol. 32, No 1, 2004.

[23] P. Walsh, P. Fletcher, GasTurbine Performance, Blackwell science 1998.

[24] A. Valera-Medina, N. Syred, P. Bowen, Central Recirculation Zone Visualization in Confined Swirl Combustors for Terrestrial Energy, Journal for Propulsion and Power, Volume 29, Number 1, 2013.

[25] M. Adzic, V. Fotev, V. Jovicic, A. Milivojevic, G. Milekic, V. Adzic, M. Bogner, Potential for Usage of Significantly Reduced Mechanisms in Numerical Modeling of Combustion Processes, FME Tran–sactions., Vol. 36, No 1, 2008.

АНАЛИТИЧКО И ЕКСПЕРИМЕНТАЛНО ИСТРАЖИВАЊЕ ИСПАРИВАЧКЕ КОМОРЕ САГОРЕВАЊА ТУРБОМЛАЗНИХ МОТОРА ЈЕДНОКРАТНЕ НАМЕНЕ

Н. Давидовић, Б. Јојић

Овај реад приказује аналитичко и експериментално истраживање испаривачке коморе сагоревања турбомлазних мотора једнократне намене. Једно–кратна употреба имплицира да су једноставност и мале димензије доминантни критеријуми.Већина емпиријских и експерименталних података комора сагоревања потиче од већих мотора и ако би их директно применили на мање коморе врло вероватно би перформансе биле прецењене. То је био један од важних разлога за ово истраживање. Аналитичка анализа је заснована на уделу испареног горива и на односу времена боравка и времена потребног за испаравање капљице са итицајем геометрије, радних услова и врсте горива. Експе–риментална анализа је фокусирана на примарну и секундарну зону, њену стабилности и ефикастност. Овај рад комбинује аналитичко и експериментално истраживање једне такве димензионо ограничене коморе са центалним испаривачем.